Communications

Indirect Observation of Structured Incipient Zeolite Nanoparticles in Clear Precursor Solutions[**]

Lubomira Tosheva,* Boriana Mihailova, Lik H. Wee, Biliana Gasharova, Krassimir Garbev, and Aidan M. Doyle*

The structure of the zeolite precursor particles present in clear synthesis solutions yielding colloidal silicalite-1 (purely siliceous zeolite with MFI-type structure) is one of the most controversial issues in modern zeolite science. Owing to the nature of the synthesis and the absence of Al, these systems are widely used as models to study the mechanism of zeolite crystallization in general. Ever since the "nanoslab" hypothesis was proposed by Martens et al.[1] it has been the subject of a lot of criticism. The major disagreement is about the structure of the subcolloidal precursor particles present in the initial clear mixtures. Whereas Martens et al. suggest that these particles have MFI structural features, an amorphous nature of the particles has been proposed in numerous other studies.[2–8] In some cases, the nanoparticles were extracted from the synthesis solutions, and concerns have been raised about possible changes in their structure or interference from the extraction procedure.[1,2,5] Other authors base their arguments against the crystalline nature of the precursor particles on the results of solid-state NMR analysis after ^{29}Si enrichment.[3,4] A recent NMR study on aqueous silicate solutions revealed the presence of structural units typical of the MFI structure.[9] Other complementary techniques such as dynamic light scattering have also been used to further characterize the species present in the precursor solu-tions.[10,11] Thus, despite the fact that a remarkable number of papers discussing the structure of the silicalite-1 precursor particles have already been published, the discussion is still ongoing and new publications regularly appear.

Infrared spectroscopy has also extensively been used to study the structure of the silicalite-1 precursor particles.[1b,5,7,12,13] Based on the presence of a band near 550 cm^{-1}, which is widely accepted to be characteristic of the MFI structure,[14] either crystalline[1b,12] or amorphous character of the precursor particles has been suggested.[5,7,13] These IR studies were performed on freeze-dried samples,[12,13] extracted precursor particles,[1b,5] and original sols.[7] However, the IR spectra published so far showed substantial differences in the 1000–1300 cm^{-1} spectral range which indicate that specific sampling affects the structural features of the nanoparticles. Recently, IR spectroscopy with synchrotron radiation was used for the first time to study in situ catalytic reactions in zeolite crystals.[15]

On the basis of synchrotron-based grazing-incidence reflection-absorption infrared (RAIR) spectra of ultrathin zeolite films on Au surfaces, we give unambiguous evidence for the existence of incipient zeolite nanoparticles in clear precursor solutions: these are subcolloidal particles having all the structural features of the zeolite framework but a size of only a few unit cells which is insufficient to generate a diffraction pattern. The novelty in our study is twofold: sample preparation and method of characterization. First, to separate the subnanoparticles from the solution, we used the Langmuir–Blodgett (LB) method to deposit them on Au substrates. The LB method allows concentration of the subcolloidal particles at the air/water interface as floating films and transfer of these films to the solid supports, which ensures preservation of the native particle structure. Second, we prepared the LB films on Au surfaces in order to characterize the samples by RAIR spectroscopy, which is the most efficient spectroscopic method for structural analysis of ultrathin films. Vibrational spectroscopy has great advantages over diffraction methods in detecting crystalline particles with a size of just 2–3 unit cells, because such particles are large enough to generate phonon modes of the corresponding crystal lattice but too small to give rise to detectable Bragg reflections even when synchrotron X-ray radiation is used. In addition, the vibrational spectra are easy to interpret and can unambiguously distinguish between amorphous and crystalline features, which is sometimes a problem for other surface-sensitive spectroscopic methods. Enhancement of the IR absorption due to the presence of a strongly reflecting noble metal surface allows the detection of even monomolecular layers when grazing-incident RAIR spectroscopy is

[*] Dr. L. Tosheva, L. H. Wee, Dr. A. M. Doyle
Division of Chemistry and Materials
Manchester Metropolitan University
Chester St., Manchester M15GD (UK)
Fax: (+44) 161-247-6357
E-mail: l.tosheva@mmu.ac.uk
a.m.doyle@mmu.ac.uk

Prof. B. Mihailova
Mineralogisch-Petrographisches Institut, Universität Hamburg
Grindelallee 48, 20146 Hamburg (Germany)

Dr. B. Gasharova
ANKA/Institute for Synchrotron Radiation, Forschungszentrum Karlsruhe
P.O. Box 3640, 76021 Karlsruhe (Germany)

Dr. K. Garbev
Institute of Technical Chemistry, Forschungszentrum Karlsruhe
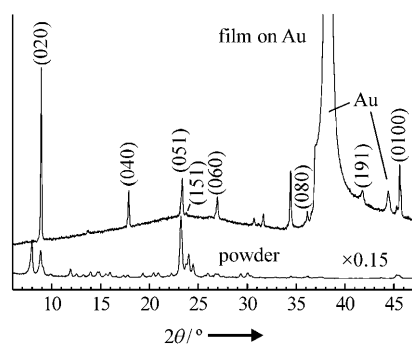P.O. Box 3640, 76021 Karlsruhe (Germany)

used.[16] Utilization of the synchrotron IR source ensured acquisition of the highest quality RAIR spectra.

We analyzed three types of silicalite-1 films obtained by various methods: 1) LB films of subcolloidal particles, 2) secondary growth of the films prepared in 1), and 3) spin coating of the clear precursor solutions. The films obtained by secondary growth after LB deposition were high-density monolayers built up from twin crystals with a typical MFI morphology and a size of about 700–800 nm (Figure 1). Their
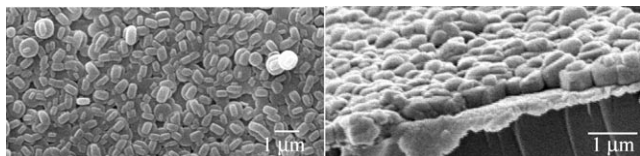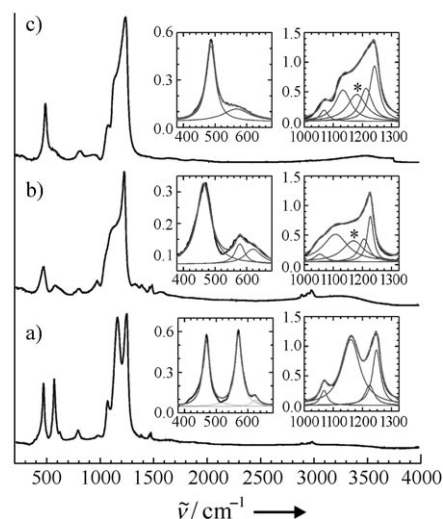

Figure 1. Scanning electron microscopy (SEM) images of as-made silicalite-1 films prepared by secondary growth of Au substrates LB-seeded by using the TEOS–CTAB solution.

high degree of crystallinity was revealed by the pronounced silicalite-1 Bragg reflections in the XRD pattern (Figure 2). The enhanced intensity of the (0k0) Bragg reflections in the

Figure 3. RAIR spectra of a) an as-made silicalite-1 film after secondary growth of LB-seeded (TEOS–CTAB solution) substrates, b) an as-made spin-coated film prepared from the TEOS–CTAB solution, and c) a calcined spin-coated film prepared from TEOS–CTAB solution. The insets show Lorentzian fits of the corresponding spectral ranges. The asterisks indicate the additional peak in the spectra of the spin-coated films.

Figure 2. XRD pattern of the as-made film prepared by secondary growth of Au substrates LB-seeded by using the TEOS–CTAB solution. Indexing is based on MFI-type structure, space group *Pnma*, and structure refinement by assuming 80% preferred (010) orientation. The enhanced background near $2\theta = 22$–23° is most probably due to the glass substrate. A typical XRD pattern of silicalite-1 powder is given for comparison.

XRD pattern indicates that the film has a preferred orientation relative to the support. The secondary grown film with verified crystallinity and density was further used as a reference sample in the RAIR spectroscopic analysis. Its RAIR spectrum is shown in Figure 3a. The peak near 550 cm^{-1} is well pronounced and the ratio of the IR absorption near 550–650 cm^{-1} to that near 440–480 cm^{-1} is even higher than the value of 0.72 considered as indicative of fully crystalline MFI zeolites.[14] Note that the intensity ratios measured in IR transmittance on KBr pellets cannot be compared straightforwardly to those measured by RAIR spectroscopy, because the latter technique is selective for vibrational modes with induced dipole moments having a

nonzero component perpendicular to the surface.[16] Also, because of specific phonon–photon interaction phenomena near the metal surface, RAIR spectral bands are observed at higher frequencies compared to those measured in IR transmittance. In addition, the peak intensities and positions of MFI films on Au surface vary with the film thickness due to grain–grain interactions during film growth and the associated elastic tension in the Si–O network.[17]

Next, we considered the RAIR spectra of films obtained by spin coating of clear precursor solutions (Figure 3b and c). Although the thickness of the films (ca. 150 nm) was sufficient to generate measurable XRD patterns, the absence of resolved Bragg reflections indicated a very small size of the crystalline coherent scattering domains. However, RAIR spectroscopy reveals the existence of zeolite crystallites in the spin-coated films. Analysis of the range 400–650 cm^{-1} clearly shows the presence of the peak near 550 cm^{-1} which is the commonly used indicator for the silicalite-1 structure.[14] So far, the small peak near 625 cm^{-1} in the spectra of the as-made samples has not been discussed in detail in the literature, because in transmittance IR spectra it overlaps with the much stronger peak at 550 cm^{-1} and appears only as a shoulder.

The peak broadening observed for the spin-coated films can be due to several factors: 1) phonon confinement effects; the small size of the particles suggests a strong impact of particle–particle interaction on the bulk phonons due to the close particle packing in the formed film; 2) possible partial damage of the zeolite subnanoparticles during the coating procedure; and 3) deposition of subnanoparticles with both well-developed and poor MFI structures from the clear TEOS–CTAB solution. The intensity ratio $\rho = [I(550) + I(620)]/I(470)$ is 1.20 for the secondary grown film and 0.39 and 0.47 for the as-made and calcined spin-coated films,

respectively. The ρ value is lower for the spin-coated films, but nevertheless it indicates the presence of zeolite nanocrystallites. The peak near 550 cm^{-1} arises from five-membered SiO$_4$ rings and, precisely speaking, it is indicative of the presence of precursor secondary building units (pentasil Si–O rings), rather than crystalline zeolite structure.[9] Using this peak, one can hardly distinguish an amorphous Si–O network which contains a number of randomly distributed five-membered SiO$_4$ rings from a system composed of many small zeolite particles with a mean size of just a few unit cells. In the former case, peak broadening will occur due to the structural disorder of the amorphous system.[18] In the latter case, peak broadening results from the very small size of the crystalline particles and associated phonon confinement effects.[19] On the other hand, crystalline Si–O networks, both dense and porous silica structures, are unambiguously distinguishable from amorphous silica by the presence of an IR peak near 1230 cm^{-1}.[5,7,14,20,21] This peak is indicative of the presence of translational symmetry in the silicon–oxygen network and therefore may serve as an even better indicator for the existence of zeolite subnanoparticles when other crystalline dense silica phases are not present. This is especially important for analyzing zeolite films. Surface-sensitive techniques such as attenuated total reflection (ATR) and RAIR are usually applied in this case, but due to the optical window of the utilized ATR crystals and the limited spectral range of sensitivity of mercury cadmium telluride (MCT) detectors used with IR microscopes, often the range below 600 cm^{-1} cannot be satisfactorily measured. Additionally, the IR absorption is twice as high in the range 900–1300 cm^{-1} as compared to the range 400–650 cm^{-1}, which increases the probability of detecting ultrathin zeolite films. Comparison of the spectra of the secondary grown and spin-coated films in the spectral range 900–1300 cm^{-1} strongly supports these arguments (Figure 3). The band near 1230 cm^{-1} is well pronounced in the spectra of both types of films and thus indicates the presence of MFI crystallites. However, an additional peak near 1170 cm^{-1} is observed for the spin-coated films, which reveals the presence of non-zeolitic, most probably noncrystalline structural species. This is in agreement with the value of the intensity ratio ρ, which is smaller for spin-coated films than for secondary grown film.

Finally, we considered the RAIR spectra of films prepared by the LB method. We could not detect RAIR signals below 800 cm^{-1} and we focused our attention on the more intense bands in the range 900–1300 cm^{-1}. The remarkable result is that the RAIR profile of the LB film synthesized without CTAB is the same as that of the highly crystalline (confirmed by XRD) and dense (confirmed by SEM) film obtained by secondary growth (Figure 4). No additional peak was necessary to fit the spectrum profile, contrary to the spin-coated films (Figure 3). This unambiguously proves that incipient crystalline zeolite subnanoparticles do exist in clear synthesis solutions.

The LB films synthesized with CTAB also show a peak near 1230 cm^{-1}, and the intensity ratio $I(1230)/I(1130)$ is similar to that of LB films synthesized without CTAB. Interestingly, the signal from the zeolite LB film was detected even with a conventional thermal IR source (Globar). This
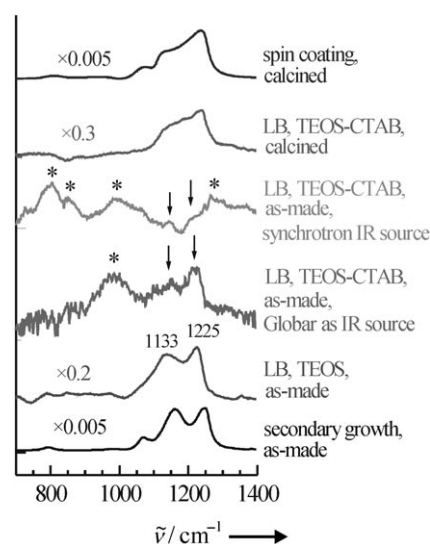
Figure 4. RAIR spectra of films synthesized by the LB method compared to the spectrum of the secondary grown film. The arrows in the spectra of as-made LB films from TEOS–CTAB indicate the MFI peaks; the asterisks mark the peaks arising from CTAB molecules.

shows that conventional RAIR experiments are very suitable to examine the efficiency of synthesis methods for growth of ultrathin zeolite film. On the other hand, the peaks arising from CTAB are enhanced when synchrotron IR radiation is used, that is, CTAB molecules are preferably oriented perpendicular to the Au surface. The latter observation also highlights the strength of synchrotron-based RAIR spectroscopy to analyze the orientation of very thin films and molecular species, due to the intrinsic collimation of synchrotron radiation and hence a better confined angle of grazing incidence than that for the Globar source. Consequently, the intensity of modes with a dipole moment perpendicular to the Au surface is much more enhanced when synchrotron radiation is used as compared to Globar. The fitting of the spectral profile of calcined LB films required an additional peak between 1130 and 1230 cm^{-1}, similar to spin-coated films. This indicates possible partial destruction of the incipient zeolite particles due to removal of the organic template. However, the fact that the peak near 1230 cm^{-1} is still well pronounced points to the overall stability of the zeolite subnanoparticles. Comparing the spectra of LB and spin-coated films showed that the LB technique allows "extraction" of the incipient zeolite nanoparticles, whereas in the spin-coated films these particles coexist with noncrystalline/poorly crystalline spatial regions.

In summary, the RAIR spectra of LB films on Au surfaces unambiguously show the existence of incipient zeolite nanoparticles in the clear silicalite-1 synthesis solutions. The approach can be applied to study the structure of the precursor species present in clear solutions used to prepare other colloidal zeolites such as zeolite Y.[22] The RAIR technique is a very appropriate analytical method to probe the structure of ultrathin zeolite films. The existence of a well-pronounced peak near 1230 cm^{-1} with intensity comparable or higher than that of the peak near 1130 cm^{-1} is indicative of the silicalite-1 structure.

Experimental Section

The clear silicalite-1 precursor solution was prepared from tetraethoxysilane (TEOS, 98%, Lancaster), tetrapropylammonium hydroxide (1.0 M solution, Aldrich), and distilled water. The mixture was placed overnight on an orbital shaker to allow hydrolysis of TEOS. The molar composition of the solution was 9 TPAOH:25 SiO_2:480 H_2O:100 EtOH (TEOS solution), where the presence of ethanol is due to the use of TEOS. Another synthesis solution with molar composition 9 TPAOH:25 SiO_2:480 H_2O:200 EtOH:0.0041 CTAB (TEOS–CTAB solution) was prepared similarly by adding ethanol (Fisher) containing 0.7 mM of the cationic surfactant cetyltrimethylammonium bromide (CTAB, Aldrich) prior to TEOS hydrolysis. The water used in all experiments was obtained from a Synergy water purification system (Millipore) with a resistivity of 18.2 MΩ cm. 3000 µL of TEOS solution or 500 µL of TEOS–CTAB solution was spread by microsyringe on the water subphase in a Langmuir–Blodgett (LB) trough (NIMA 1232D1D2, NIMA Technology). The floating films were compressed to 10 mN m^{-1} (TEOS solution) or 15 mN m^{-1} (TEOS-CTAB solution) at a speed of 50 cm^2 min^{-1}, and the films were transferred to gold coated glass slides (100 nm Au layer with Ti adhesive layer, Sigma-Aldrich) by the vertical lifting method at a dip speed of 1 mm min^{-1}. The Au substrates were precut with diamond wire to 1 cm × 1 cm pieces, cleaned in an ultrasonic bath with acetone and 2-propanol and thoroughly rinsed with distilled water prior to film preparation. LB samples prepared from TEOS–CTAB solution were sintered at 500 °C for 1 h in a preheated furnace and used to prepare silicalite-1 films by secondary growth. The synthesis solution for secondary growth had the molar composition 3 TPAOH:25 SiO_2:1500 H_2O:100 EtOH and was prepared similarly to TEOS solution. The LB-seeded Au substrate was mounted vertically in a polypropylene reactor and treated under reflux in an oil bath at 100 °C for 24 h. After synthesis, the sample was separated from the mother liquor, ultrasonically treated in 0.1 M ammonia solution for 10 min, rinsed with distilled water, and dried at 60 °C. Spin-coated zeolite films were also prepared from clear TEOS–CTAB precursor solution with a G3P-8 spin coater (PI-KEM) at a spinning rate of 3000 rpm for 60 s. The spin-coated films were dried at 60 °C and optionally calcined at 550 °C for 4 h.

The morphology of the films was studied by SEM (JEOL 5600LV) and atomic force microscopy (Digital Instruments D3100 AFM, Veeco Instruments Inc., Santa Barbara, operated in tapping mode). XRD patterns of secondary grown films were collected on an X'Pert MPD PRO diffractometer by using Ni beta-filtered Cu$_{K\alpha}$ radiation and an X'Celerator real time multiple strip detector. The XRD data were evaluated with the Bruker-AXS software Diffrac*Plus* 13.0 and the ICDD 2002 database.

Synchrotron-based RAIR spectroscopic experiments were conducted at the IR beamline of the 2.5-GeV synchrotron facility ANKA, Karlsruhe. The spectra were measured with a Bruker IFS 66v/S spectrometer coupled to a Bruker IRscope II microscope equipped with a double-pass 15 × Schwarzschild-based grazing-angle objective having an angle of incidence of about 83° and numerical aperture of 0.4. The spectra were collected in an N_2-purged enclosure box (humidity < 3%) by using p-polarized light selected with gold-grid and KRS-5 polarizers for the far- and mid-IR range, respectively, and instrument resolution of 2 cm^{-1}. RAIR spectra in the far-IR range of 200–700 cm^{-1} were recorded with a liquid-He-cooled (4.2 K) Si bolometer detector (Infrared Laboratories, Inc., USA) and a 6 µm Si/Mylar beam splitter, while for the mid-IR range of 650–4000 cm^{-1} a liquid-N_2-cooled MCT detector (InfraRed Associates Inc., Stuart, FL) and a KBr beam splitter were used. Due to the grazing-angle geometry, the beam spot on the sample surface was elliptically shaped with approximate dimensions of 500 × 120 µm. To eliminate the influence of the decay of the synchrotron electron beam current, a background spectrum was collected from a clean Au surface before measuring each sample spectrum.

[1] a) R. Ravishankar, C. E. A. Kirschhock, P.-P. Knops-Gerrits, E. J. P. Feijen, P. J. Grobet, P. Vanoppen, F. C. De Schryver, G. Miche, H. Fuess, B. J. Schoeman, P. A. Jacobs, J. A. Martens, *J. Phys. Chem. B* **1999**, *103*, 4960–4964; b) C. E. A. Kirschhock, R. Ravishankar, F. Verspeurt, P. J. Grobet, P. A. Jacobs, J. A. Martens, *J. Phys. Chem. B* **1999**, *103*, 4965–4971; c) C. E. A. Kirschhock, V. Buschmann, S. Kremer, R. Ravishankar, C. J. Y. Houssin, B. L. Mojet, R. A. van Santen, P. J. Grobet, P. A. Jacobs, J. A. Martens, *Angew. Chem.* **2001**, *113*, 2707–2710; *Angew. Chem. Int. Ed.* **2001**, *40*, 2637–2640.

[2] H. Ramanan, E. Kokkoli, M. Tsapatsis, *Angew. Chem.* **2004**, *116*, 4658–4661; *Angew. Chem. Int. Ed.* **2004**, *43*, 4558–4561.

[3] a) C. T. G. Knight, S. D. Kinrade, *J. Phys. Chem. B* **2002**, *106*, 3329–3332; b) C. T. G. Knight, J. Wang, S. D. Kinrade, *Phys. Chem. Chem. Phys.* **2006**, *8*, 3099–3103.

[4] C.-H. Cheng, D. F. Shantz, *J. Phys. Chem. B* **2006**, *110*, 313–318.

[5] D. D. Kragten, J. M. Fedeyko, K. R. Sawant, J. D. Rimer, D. G. Vlachos, R. F. Lobo, *J. Phys. Chem. B* **2003**, *107*, 10006–10016.

[6] T. M. Davis, T. O. Drews, H. Ramanan, C. He, J. Dong, H. Schnablegger, M. A. Katsoulakis, E. Kokkoli, A. V. Mccormick, R. Lee Penn, M. Tsapatsis, *Nat. Mater.* **2006**, *5*, 400–408.

[7] A. Patis, V. Dracopoulos, V. Nikolakis, *J. Phys. Chem. C* **2007**, *111*, 17478–17484.

[8] C. A. Fyfe, R. J. Darton, C. Shneider, F. Scheffler, *J. Phys. Chem. C* **2008**, *112*, 80–88.

[9] M. Haouas, F. Taulelle, *J. Phys. Chem. B* **2006**, *110*, 3007–3014.

[10] A. Aerts, L. R. Follens, M. Haouas, T. P. Caremans, M.-A. Delsuc, B. Loppinet, J. Vermant, B. Goderis, F. Taulelle, J. A. Martens, C. E. A. Kirschhock, *Chem. Mater.* **2007**, *19*, 3448–3454.

[11] S. Mintova, N. H. Olson, J. Senker, T. Bein, *Angew. Chem.* **2002**, *114*, 2670–2673; *Angew. Chem. Int. Ed.* **2002**, *41*, 2558–2561.

[12] S. L. Burkett, M. E. Davis, *Chem. Mater.* **1995**, *7*, 920–928.

[13] J. N. Watson, L. E. Iton, R. I. Keir, J. C. Thomas, T. L. Dowling, J. W. White, *J. Phys. Chem. B* **1997**, *101*, 10094–10104.

[14] G. Coudurier, C. Naccache, J. C. Vedrine, *Chem. Commun.* **1982**, 1413–1415.

[15] E. Stavitski, M. H. F. Kox, I. Swart, F. M. F. de Groot, B. M. Weckhuysen, *Angew. Chem. Int. Ed.* **2008**, *47*, 3543–3547.

[16] a) M. Urban, J. Koenigin in *Vibrational Spectra and Structure: A Series in Advances. Vol. 18, Applications of FT-IR spectroscopy* (Ed.: J. R. Durig), Elsevier, New York, **1990**, pp. 127–181; b) R. G. Greenler, *J. Chem. Phys.* **1966**, *44*, 310–315.

[17] B. Mihailova, V. Engström, J. Hedlund, A. Holmgren, J. Sterte, *Microporous Mesoporous Mater.* **1999**, *32*, 297–304.

[18] F. L. Galeener, P. N. Sen, *Phys. Rev. B* **1978**, *17*, 1928–1933.

[19] G. Gouadec, P. Colomban, *Prog. Cryst. Growth Charact. Mater.* **2007**, *53*, 1–56.

[20] B. J. Schoeman, O. Regev, *Zeolites* **1996**, *17*, 447–456.

[21] S. P. Zhdanov, L. S. Kosheleva, T. I. Titova, *Langmuir* **1987**, *3*, 960–967.

[22] S. Mintova, N. H. Olson, T. Bein, *Angew. Chem.* **1999**, *111*, 3405–3408; *Angew. Chem. Int. Ed.* **1999**, *38*, 3201–3204.